Stem Cell Research 16 (2016) 541–551

Contents lists available at ScienceDirect

Stem Cell Research

journal homepage: www.elsevier.com/locate/scr

Highly efficient generation of glutamatergic/cholinergic NT2-derived postmitotic human neurons by short-term treatment with the nucleoside analogue cytosine β-D-arabinofuranoside

Imanol González-Burguera [a], Ana Ricobaraza [a], Xabier Aretxabala [b], Sergio Barrondo [a,c], Gontzal García del Caño [b,*], Maider López de Jesús [a,c,**], Joan Sallés [a,c]

[a] Department of Pharmacology, Faculty of Pharmacy, University of the Basque Country (UPV/EHU), Paseo de la Universidad 7, 01006 Vitoria-Gasteiz (Araba), Spain
[b] Department of Neurosciences, Faculty of Pharmacy, University of the Basque Country (UPV/EHU), Paseo de la Universidad 7, 01006 Vitoria-Gasteiz (Araba), Spain
[c] CIBERSAM, Spain

ARTICLE INFO

Article history:
Received 14 May 2015
Received in revised form 25 January 2016
Accepted 26 February 2016
Available online 3 March 2016

Keywords:
Pluripotent NT2 cells
Retinoic acid
Cytosine β-D-arabinofuranoside
Neuronal differentiation
Postmitotic human neurons
Neurotransmitter phenotype

ABSTRACT

The human NTERA2/D1 (NT2) cells generate postmitotic neurons (NT2N cells) upon retinoic acid (RA) treatment and are functionally integrated in the host tissue following grafting into the rodent and human brain, thus representing a promising source for neuronal replacement therapy. Yet the major limitations of this model are the lengthy differentiation procedure and its low efficiency, although recent studies suggest that the differentiation process can be shortened to less than 1 week using nucleoside analogues. To explore whether short-term exposure of NT2 cells to the nucleoside analogue cytosine β-D-arabinofuranoside (AraC) could be a suitable method to efficiently generate mature neurons, we conducted a neurochemical and morphometric characterization of AraC-differentiated NT2N (AraC/NT2N) neurons and improved the differentiation efficiency by modifying the cell culture schedule. Moreover, we analyzed the neurotransmitter phenotypes of AraC/NT2N neurons. Cultures obtained by treatment with AraC were highly enriched in postmitotic neurons and essentially composed of dual glutamatergic/cholinergic neurons, which contrasts with the preferential GABAergic phenotype that we found after RA differentiation.

Taken together, our results further reinforce the notion NT2 cells are a versatile source of neuronal phenotypes and provide a new encouraging platform for studying mechanisms of neuronal differentiation and for exploring neuronal replacement strategies.

1. Introduction

The pluripotent NTERA2/D1 (NT2) cell line, derived from human testicular embryonic carcinoma cells (Andrews, 1984), represents a committed neuronal precursor cell that can be induced to differentiate *in vitro* into postmitotic cells, known as NT2N (or hNT) neurons. Moreover, NT2N cells have the ability to establish functional synapses and to develop neuronal electrophysiological properties, including generation of action potentials and the presence of spontaneous excitatory and inhibitory postsynaptic currents (Hartley et al., 1999a; Podrygajlo et al., 2010; Öz et al., 2013). Consequently, the NT2N cell type is now widely accepted as a suitable model for the study of neuronal networks and differentiation and synaptogenesis processes.

In addition, the NT2 clonal line represents a promising cell source for neuronal replacement therapy applicable to the treatment of some neurological conditions, including neurodegenerative disorders such as Parkinson's, Huntington's, and Alzheimer's diseases and acute brain injury such as stroke and head trauma. To this end, grafts or cells in suspension from embryonic ventral mesencephalic tissue, adrenal medullary cells, other neuronal and non-neuronal cells, and even genetically modified cells have produced encouraging results, but none of them are fully satisfactory (Martínez-Morales et al., 2013). As a consequence, researchers have focused their efforts on either trying to increase the efficacy of existing tissue and cell candidates or searching for alternative sources of donor cells. In this sense, NT2N neurons maintain their neuronal phenotype after transplantation into the rodent brain (Trojanowski et al., 1993; Kleppner et al., 1995; Baker and

* Correspondence to: G. García del Caño, Department of Neurosciences, Faculty of Pharmacy, University of the Basque Country (UPV/EHU), Paseo de la Universidad 7, 01006 Vitoria-Gasteiz (Araba), Spain.
** Correspondence to: M. López de Jesús, Department of Pharmacology, Faculty of Pharmacy, University of the Basque Country (UPV/EHU), Paseo de la Universidad 7, 01006 Vitoria-Gasteiz (Araba), Spain.
E-mail addresses: imanol.gonzalezb@ehu.eus (I. González-Burguera), analourdes.ricobaraza@ehu.eus (A. Ricobaraza), xabier.arechabala@ehu.eus (X. Aretxabala), sergio.barrondo@ehu.eus (S. Barrondo), gontzal.garcia@ehu.eus (G. García del Caño), maider.lopez@ehu.eus (M. López de Jesús), joan.salles@ehu.es (J. Sallés).

http://dx.doi.org/10.1016/j.scr.2016.02.038
1873-5061/

Mendez, 2005) and spinal cord (Hartley et al., 1999b; Lee et al., 2000). Furthermore, NT2N grafts have been shown to improve motor deficits in animal models of stroke (Borlongan et al., 1998a,b; Saporta et al., 1999) and Huntington's disease (Hurlbert et al., 1999), making NT2N neurons excellent candidates for cell replacement therapy in neurological disorders (Trojanowski et al., 1997; Lee et al., 2000; Nelson et al., 2002; Borlongan et al., 2006; Hara et al., 2008). Indeed, in a phase I clinical trial on 12 patients with basal ganglia stroke and stable motor deficits, NT2N cells were seen to integrate with the host brain tissue for long periods and with no detectable tumor formation (Kondziolka et al., 2000; Meltzer et al., 2001; Nelson et al., 2002), leading to a Phase II study in 18 patients with basal ganglia infarct (Kondziolka et al., 2005). Although statistical significance could not be reached due to the small population size analyzed, both studies showed an apparent trend towards functional improvement (Banerjee et al., 2010, for review).

Progress in the field of neuronal replacement using NT2 committed to differentiate with retinoic acid (RA) is limited by the long time frame necessary to generate postmitotic NT2N neurons and also by the low proportion of terminally differentiated neurons. Thus, neuronal differentiation of NT2 progenitors, first described by Andrews (1984) and later on improved by Pleasure et al. (1992), involves treatment of NT2 progenitors with RA during 4 weeks followed by mitotic inhibitors for 7–10 days, with only about 5% of the initial population of NT2 cells becoming differentiated. Recently, using nucleoside analogues, Musch et al. (2010) achieved successful differentiation of NT2 cells in less than 1 week, thus offering a rapid protocol to obtain postmitotic neurons, which could be potentially useful for neuronal replacement therapy. However, whereas NT2N neurons obtained by treatment with RA have been shown to express a variety of classical neurotransmitters, neurotransmitter-related enzymes and transporters (Podrygajlo et al., 2009; Coyle et al., 2011), there are no published data about neuronal phenotypes resulting from nucleoside-induced differentiation of NT2 cells.

In this study, using neuron-specific and neurotransmitter phenotype markers, high-resolution fluorescence microscopy, and western blot analysis, we demonstrate that NT2 progenitors can be committed to differentiate into NT2N neurons with high efficiency by short-term (6 days) exposure to the nucleoside analogue cytosine β-D-arabinofuranoside (AraC). AraC-differentiated neurons are irreversibly postmitotic, express late neuronal markers, are morphometrically identifiable and display a dual glutamatergic/cholinergic neurotransmitter phenotype, which differs from that observed in RA-differentiated NT2N neurons. Our data, further confirm that NT2 progenitors constitute a versatile source of neurons with a potential use in cell-replacement therapy for multiple degenerative disorders.

2. Materials and methods

2.1. Cell culture and differentiation

Human teratocarcinoma NTERA2-D1 (hereafter referred to as NT2) cells from the American Type Culture Collection (ATCC®, CRL-1973™) were maintained in complete medium (Dulbecco's Modified Eagle medium (DMEM®), ATCC 30-2002™- supplemented with 10% fetal bovine serum (FBS), Sigma-Aldrich, St Louis, MO, USA; and antibiotics, 100 U/mL penicillin and 100 μg/mL streptomycin, Gibco, Life Technologies S.A., Madrid, Spain) at 37 °C under a humidified atmosphere containing 5% CO_2. For differentiation of NT2 progenitors with all-trans retinoic acid (RA, Sigma-Aldrich), cells were treated as previously described by Pleasure et al. (1992), thus obtaining RA-differentiated NT2N cells, which will be referred to as RA/NT2N cells in this paper (see supplementary material and methods for details).

The induction of neuronal differentiation using 2′-deoxy-5-azacytidine (DAC) or cytosine β-D-arabinofuranoside (AraC) was performed based on a previous report showing that exposure of NT2 cells for only 6 days leads to neuronal differentiation (Musch et al., 2010). For preliminary assays, progenitor NT2 cells were exposed to equitoxic concentrations of DAC or AraC (Tan et al., 2007; Musch et al., 2010). Briefly, NT2 cells at 80–90% confluence were treated with 1 μM DAC or 20 μM AraC-containing medium for 24 h, 48 h, 72 h, or 6 days. Medium from cultures treated for more than 48 h was replaced with fresh complete medium supplemented with the corresponding nucleoside analogue every 2 days. Results of preliminary experiments led us to choose AraC to induce neuronal differentiation (see results below), and therefore, this compound was used for subsequent experiments. Because low cell density can compromise neuronal survival and differentiation, we tested whether increased confluence improves the yield of terminally AraC-differentiated neurons (hereafter referred to as AraC/NT2N cells). The protocol used for this purpose is described in detail in supplementary material and methods.

2.2. Western blot

Cell pellets were collected by centrifugation at different times of differentiation treatment as indicated for each experiment and lysed in homogenization buffer (10 mM Tris–HCl buffer, pH 7.4, 2 mM $MgCl_2$, and 0.32 M sucrose) containing protease inhibitors (0.5 mM iodoacetamide and 1 mM phenylmethylsulfonyl fluoride, PMSF). Depending on the antigen to be analyzed, different amounts of denatured lysates (5–30 μg) were loaded, resolved by SDS–polyacrylamide (SDS–PAGE) gels and transferred to polyvinylidene fluoride membranes (Bio-Rad, Madrid, Spain), and specific protein bands were detected using conventional immunoblot protocols. Primary and secondary antibodies are described in Table 1 and Table S1, respectively (further information about immunoblot analysis is provided as supplementary material).

2.3. Immunofluorescence

Cells were fixed in buffered 4% paraformaldehyde for 4 min, both at 20°–25 °C. After blocking for 1 h with gelatin-histology buffer (0.1 M PBS, pH 7.4, containing 0.22% gelatin (Panreac, Barcelona, Spain), 0.05% saponin (Sigma-Aldrich), and 1% serum albumin bovine (BSA, Sigma-Aldrich), cells were incubated with primary antibodies (Table 1, for details) at 4 °C overnight. Then, the appropriate fluorescent dye-conjugated secondary antibodies (Table S1 for details) were applied and nuclei were counterstained with Hoechst 33,342 (Sigma-Aldrich, diluted to 0.1 μg/mL in gelatin histology buffer) (see supplementary material and methods for further details).

2.4. BrdU labeling

Undifferentiated NT2 progenitors and AraC-treated NT2 cultures were labeled with 10 μM 5-bromo-2′-deoxyuridine (BrdU; ThermoFisher Scientific, Barcelona, Spain) at various times after initiation of AraC treatment (0, 2, 4, 8, 20 and 68 h) and fixed for immunofluorescence labeling 4 h later. Additionally, to test whether differentiated AraC/NT2N neurons were irreversibly postmitotic, after the 6-day differentiation process, AraC-containing medium was replaced with AraC-free complete medium, and cells were treated with BrdU for either 4 or 24 h and analyzed at survival times of 7, 9, and 11 days. Antigen retrieval for BrdU staining was performed as described by Solovei et al. (2006). Briefly, coverslips containing the paraformaldehyde-fixed cells were treated with PBS (0.1 M, pH 7.4) containing 0.1% (v/v) TX-100 (PBS-T), treated with HCl 0.1 M for 10 min, and then equilibrated in Saline Sodium Citrate (SSC; 0.15 M NaCl, 0.015 M sodium citrate) at room temperature (21–23 °C). Thereafter, cells were incubated in 50% formamide in SSC during 15 min at room temperature, followed by treatment

Table 1
Primary antibodies used in this study.

Antibody	Dilution		Clonality	Species and isotype	Immunizing antigen	Source, catalog no.
	IF	WB				
NeuN	1:200	1:1000	Monoclonal	Mouse IgG_1	Purified cell nuclei from mouse brain.	Millipore, MAB377, clone A60.
Nav1.6 Nav channel	1:200		Monoclonal	Mouse IgG_1	Synthetic peptide corresponding to amino acids 459–476 of the intracellular loop I-II of rat Nav1.6.	NeuroMab, 75–026, clone K87A/10.
β-III tubulin	1:1000	1:1000	Polyclonal	Affinity-purified chicken serum	Synthetic peptides corresponding to different regions shared by human and rat β-tubulin III.	Abcam, ab41489.
NF200	1:400	1:10,000	Polyclonal	Rabbit IgGs, affinity-purified	200 kDa neurofilament, purified from bovine spinal cord.	Sigma-Aldrich, N4142.
DCX	1:200	1:500	Polyclonal	Goat IgGs, affinity-purified	Synthetic peptide mapping at the C-terminus of human doublecortin.	Santa Cruz Biotech. Inc., sc-8066.
MAP2	1:200		Monoclonal	Mouse IgG_1	Bovine MAP2. Recognizes the high molecular weight forms of MAP2, MAP2a and MAP2b.	Sigma-Aldrich, M2320, clone AP-20.
BrDU	1:250		Monoclonal	Mouse IgG_{2a}	5-Iodouridine covalently coupled to ovalbumin.	ThermoFisher Scientific, MA3-071, clone BU-1.
GAD67	1:100	1:1000	Monoclonal	Mouse IgG_{2a}	Recombinant GAD67 protein of human origin.	Millipore, MAB5406, clone 1G10.2.
ChAT	1:100	1:1000	Polyclonal	Goat serum, affinity purified	Human placental enzyme.	Millipore, AB144P.
TH	1:100	1:1000	Polyclonal	Rabbit serum, affinity purified	Denatured tyrosine hydroxylase from rat pheochromocytoma.	Millipore, AB152.
VGluT1	1:200	1:1500	Polyclonal	Rabbit IgGs, affinity-purified	Synthetic peptide from a cytoplasmic loop of rat (C-terminal) VGluT1.	Abcam, ab72311.

with 70% formamide in SSC for 2 min at 70 °C. The coverslips containing plates were placed on ice and cells were washed three times with cold PBS-T and processed for double β-III tubulin and BrdU immunofluorescence as described above.

2.5. Microscope studies and imaging

All microscope images were acquired with an epifluorescence microscope Carl Zeiss Axio Observer.Z1, equipped with an HXP120C metal halide lamp illumination source and a high-resolution monochromatic camera (AxioCam MRm, 1388 × 1040 pixels), all from Carl Zeiss MicroImaging, Inc. (Gottigen, Germany).

Conventional epifluorescence images (Figs. 5 and 6) were acquired using a 20× Plan-Apochromat objective (NA 0.8). Higher-resolution images (Figs. 2, 4, and 6 and Figs. S3–S5) were acquired using a structured illumination module (ApoTome) and a XYZ motorized stage (Carl Zeiss MicroImaging, Inc), using a 63× Plan-Apochromat objective (NA 1.4), and optical sections (0.24 μm intervals in the *z*-axis) were obtained with the Zeiss ApoTome device, with camera settings adjusted to obtain images with a pixel size of 0.01 μm^2.

2.6. BrdU-positive cell counts

Conventional epifluorescence images 447.63 × 335.40 μm of cells co-immunostained for β-III tubulin and BrdU, and counterstained for nuclei with Hoechst 33,342, were acquired using a 20× Plan-Apochromat objective. All images from each independent experiment were acquired with identical exposure and lighting conditions, and nuclei displaying BrdU staining above a set threshold level (by NIH ImageJ software) were scored as positive. Three independent experiments were performed, each with two coverslips per experimental condition. Quantifications were performed on 5–7 images per slide (10–14 per experimental condition), and the percentage of BrdU-positive cells was calculated.

2.7. Statistical analysis

Results were statistically analyzed in GraphPad Prism (version 5.0, GraphPad Software Inc., San Diego, CA) and presented as mean ± SEM. Two-tailed unpaired *t*-test or one-way analysis of variance (ANOVA) followed by Bonferroni post hoc test were used. $p < 0.05$ was considered significant. Average values were obtained from either 3 or 4 independent experiments.

3. Results

3.1. Short exposure of NT2 progenitors to AraC efficiently promotes acquisition of neuron-like morphology.

First, we reproduced the RA-induced differentiation protocol previously described by Pleasure et al. (1992) and showed that only 4.4 ± 0.8% (SEM) of the initial population become terminally differentiated into RA/NT2N neurons, in line with the observations by Pleasure et al. (1992). Subsequently, we tested the ability of DAC and AraC to promote short-term neuron-like differentiation, showing that treatment with AraC (but not DAC) for only 6 days led to differentiation of NT2 progenitors into highly polarized cells with long processes, indicative of their neuronal identity. Results of these preliminary experiments are described in detail in supplementary results and illustrated in supplementary Figs. S1 and S2.

However, despite the apparent efficacy of AraC to promote neuronal differentiation, after the 6-day period of treatment, cultures were extremely sparse. Indeed, only 42.18 ± 2.78% and 9.3 ± 1.1% of the initial cell population had survived after 72 h and 6 days of treatment, respectively. Therefore, we tested whether survival could be improved by increasing cell confluence. For this purpose, after 72 h of AraC treatment, cells were harvested, replated at higher density, and treated with AraC for 3 additional days. In fact, this procedure resulted in a 2-fold increase of surviving cells (20.2 ± 3.3% *vs.* 9.3 ± 1.1%). Fig. 1 illustrates morphological changes occurring during the first 72 h of AraC-induced differentiation (Figs. 1A–D) and the features of the culture at the end of the standard (Fig. 1E) and modified schedules (Fig. 1F). As it can be observed, both procedures yielded a culture highly enriched in cells with neuronal morphology (AraC/NT2N cells).

3.2. Treatment of NT2 cells with AraC for 6 days induces terminal neuron differentiation with high efficiency.

To ascertain whether AraC/NT2N cells expressed markers consistent with a neuronal phenotype, we analyzed the expression of the neuron-specific cytoskeletal proteins neurofilament 200 kDa (NF200), β-III tubulin, and doublecortin (DCX) during the time course of RA- and AraC-induced differentiation process, by immunoblot of whole cell

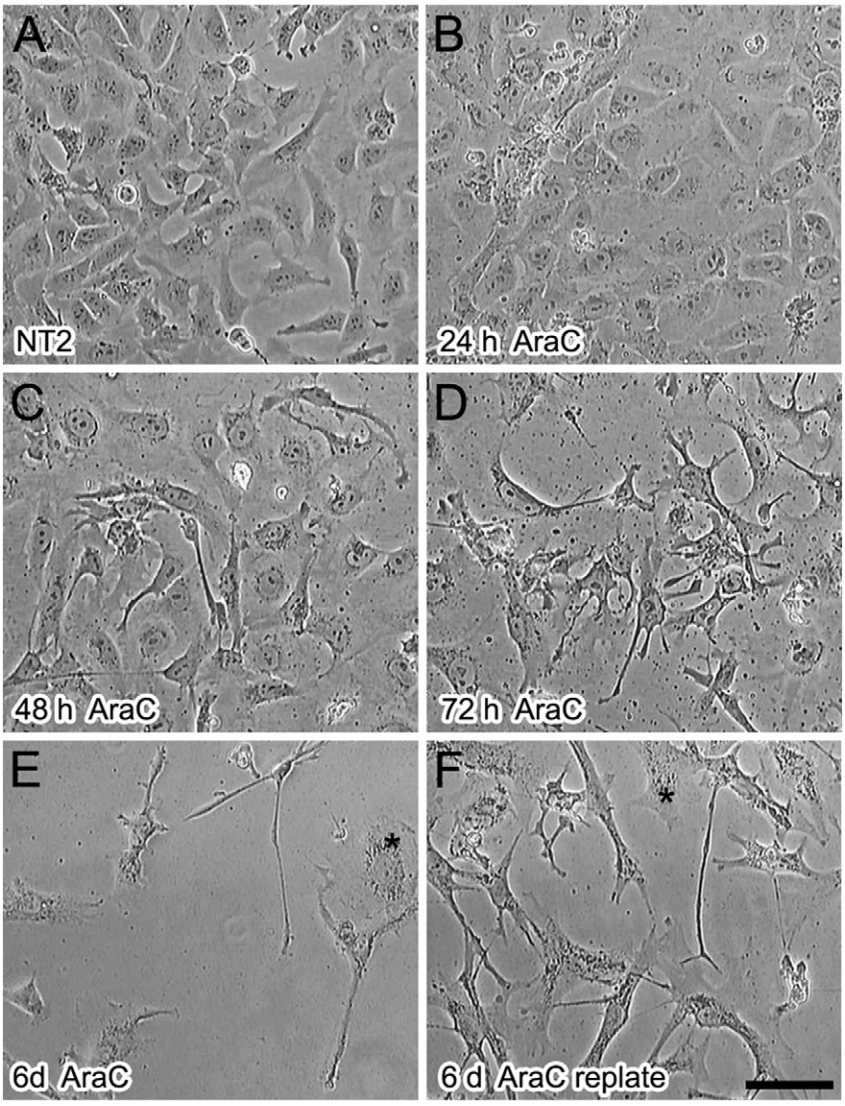

Fig. 1. Phase-contrast micrographs illustrating the time course of AraC-induced differentiation (A–E) and the effects of increasing cell confluence at 72 h of AraC treatment in the state of cultures after 6-day period of treatment (F). Asterisks indicate the presence of a population of flat cells with phase-translucent cytoplasm and non-neuronal morphology at the end of treatment. Scale bar = 50 μm (applies to A–F).

homogenates (Fig. 2A). Both RA and AraC led to an increase of NF200 expression, reaching a maximum at the end of the differentiation process, showing only subtle differences in the relative expression level during the time course of treatments. By contrast, the temporal expression profile of β-III tubulin and DCX showed marked differences between the RA and the AraC induction of differentiation. Thus, upon RA treatment of NT2 progenitors, the expression of β-III tubulin increased rapidly and then decreased, whereas it increased sharply at the end of the AraC treatment. DCX, in its turn, increased progressively in RA-treated cells, whereas it showed an up- and downregulation pattern in AraC-treated cells (Fig. 2A).

Subsequently, we performed immunolabeling experiments for β-III tubulin, NF200 and DCX in NT2 progenitors, RA/NT2N and AraC/NT2N cells (Figs. 2B–J). No or barely detectable NF200 immunolabeling was observed in NT2 cells (Fig. 2B), whereas a bright signal could be observed in both RA/NT2N (Fig. 2E) and AraC/NT2N (Fig. 2H) cells. Also in good agreement with immunoblot results (Fig. 2A), β-III tubulin immunolabeling was diffusely distributed in the cytoplasm of NT2 progenitors (Fig. 2C), whereas intense immunoreactivity was found in varicosities within the neurites of RA/NT2N cells (Fig. 2F) and throughout the cell body and neurites or AraC/NT2N cells (Fig. 2I). NT2 cells resulted diffusely stained by anti-DCX antibody, whereas it gave a strong fluorescent signal in neurites of RA/NT2N cells (Fig. 2G) and consistently delineated neurites of AraC/NT2N cells (Fig. 2J).

The neuronal identity of AraC/NT2N cells was validated by double immunofluorescence labeling for NeuN/Fox-3 (a marker of adult neurons) and β-III tubulin, in cell cultures treated with AraC for 6 days and subjected or not to replating on day 3. Results showed that AraC/NT2N cells co-express both markers (Figs. S3A–G), along with MAP2 and the voltage-dependent sodium channel 1.6 (Nav 1.6) (Fig. S4).

Because cultures of NT2 cells treated for 6 days with AraC still contained a population of presumably non-neuronal cells, NeuN/Fox-3 staining, together with morphological features, was used to evaluate the efficiency of both schedules to induce neuronal differentiation. For this purpose, we performed cell counts on cell cultures doubly immunolabeled for NeuN/Fox-3 and β-III tubulin, and cells negative for NeuN/Fox-3 and those displaying round shapes with no or short processes were considered to be non-neuronal. Using

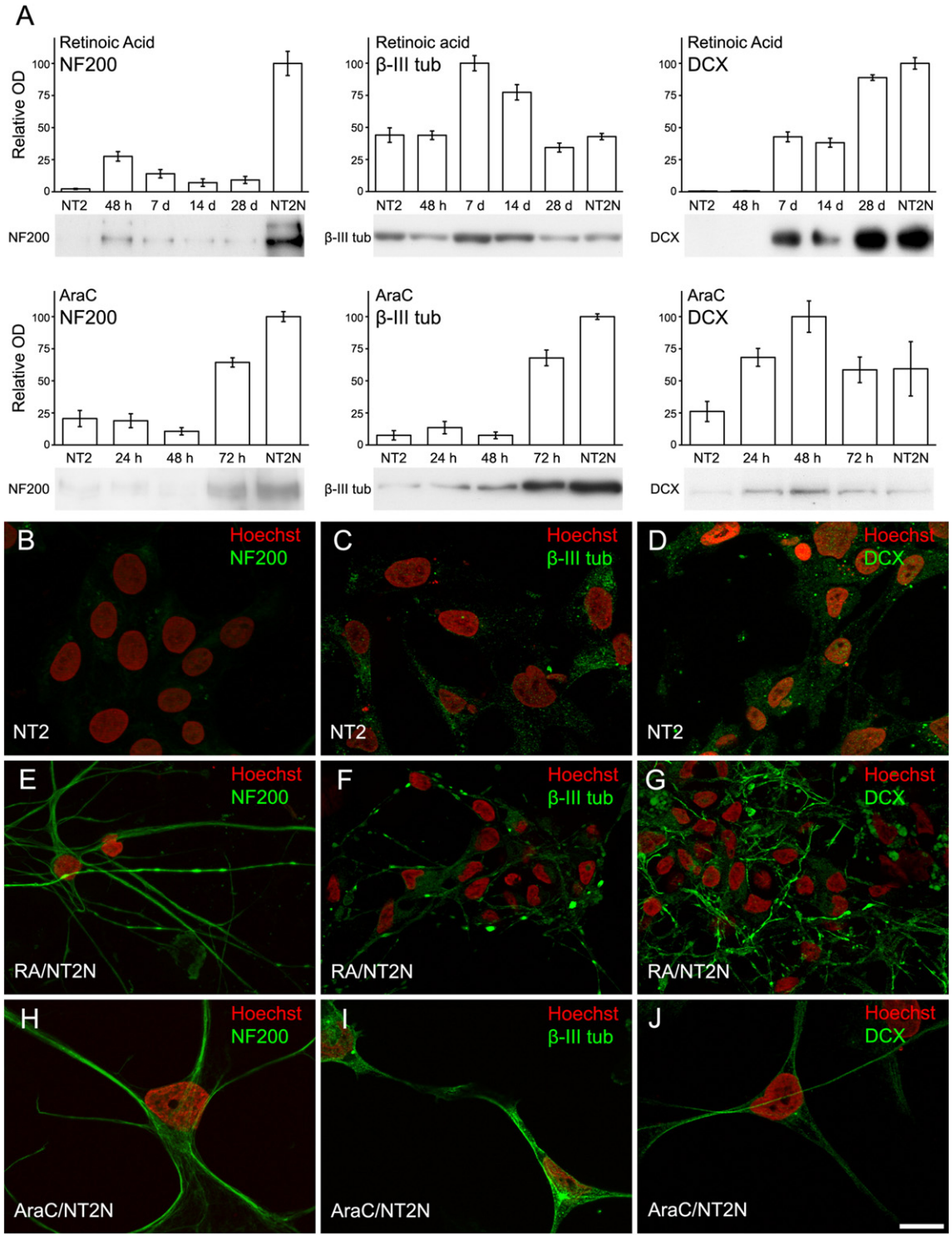

Fig. 2. (A) Results of immunoblots and semiquantitative densitometric analysis of immunoreactivity for neuronal markers NF200, β-III tubulin, and DCX during RA- and AraC-induced differentiation. Immunoblots were performed in whole homogenates of cells harvested at different time points of differentiation using RA (NT2 progenitors, 48 h, 7 days, 14 days, and 28 days and terminally differentiated RA/NT2N neurons) and AraC (NT2 progenitors, 24 h, 48 h, and 72 h and terminally differentiated AraC/NT2N neurons). The amount of protein loaded per lane was 5 μg for immunoblots against NF200 and β-III tubulin and 20 μg for immunoblots against DCX. The *y*-axis of graphs show percent optical density of each band normalized to the highest value found during the time course of differentiation. Error bars indicate SEM ($n = 4$). B. Micrographs of NT2 cells (B–D) and terminally differentiated RA/NT2N (E–G) and AraC/NT2N (H–J) neurons immunolabeled (green) for NF200 (B, E, H), β-III tubulin (C, F, I) and DCX (D, G, J) combined with chromatin staining using the Hoechst's dye (pseudocolored red). Micrographs are maximum intensity projections of 4 consecutive optical sections separated by 0.24 μm, obtained using the structured illumination module (ApoTome) of a fluorescence microscope (Carl Zeiss Axio Observer) equipped with a XYZ motorized stage. Scale bar = 20 μm (applies to B–J).

these criteria, we concluded that 55.4 ± 2.4% of cells exposed to uninterrupted 6-day treatment and 71.3 ± 3.9% of cells subjected to replating on day 3 fulfilled criteria to be considered as AraC/NT2N neurons. Using these values and the percentage of surviving cells following 6 days of treatment with AraC (see above), we could conclude that 5.14 ± 0.6% and 14.4 ± 2.3% of the initial population of NT2 progenitors became terminally differentiated AraC/NT2N neurons (Fig. S3H).

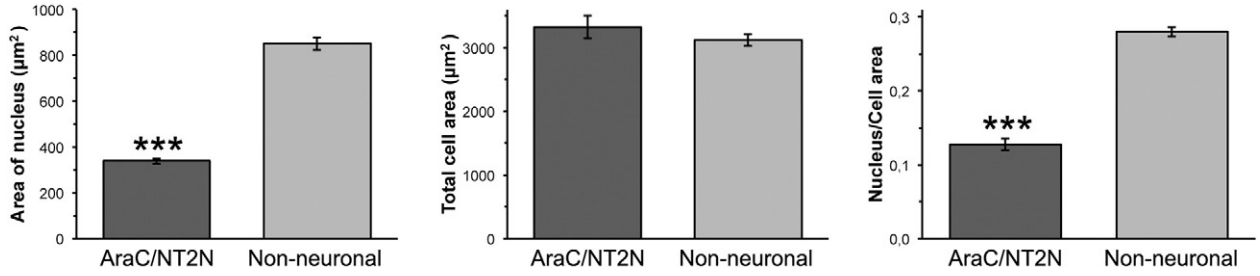

Fig. 3. Bar graphs showing results of morphometric analyses to compare non-neuronal and AraC/NT2N cells grown in identical conditions. All data represent average values obtained from 99 cells in 3 independent experiments. Data are mean ± SEM. Two-tailed unpaired *t*-test (***$p < 0.0001$).

Collectively, these results demonstrate the effectiveness of AraC to promote neuronal differentiation of NT2 cells in a short time period and highlight the importance of optimizing culture conditions.

3.3. Cells identified as AraC/NT2N neurons are morphometrically distinguishable from non-neuronal cells

To assess whether phenotypes classified as neuronal and non-neuronal after AraC-induced differentiation were morphometrically distinguishable, we analyzed the average nuclear and whole cell area of both cell populations, classified on the basis of NeuN/Fox-3 expression and morphological features (González-Burguera et al., in press for details). The average nuclear area of cells classified as non-neuronal, was considerably larger (851.53 ± 27.63 µm^2) than nuclear area of AraC/NT2N neurons (339.67 ± 11.91 µm^2), whereas no differences in total cell area were observed (3122.36 ± 95.06 and 3326.82 ± 177.68 µm^2, respectively). Consequently, the ratio of nuclear area to total cell body area was about 2-fold higher in non-neuronal cells (0.280 ± 0.007) than in AraC/NT2N cells (0.128 ± 0.008) (Fig. 3). These results clearly reinforce the reliability of criteria used to classify cell phenotypes resulting from exposure of NT2 progenitors to AraC treatment.

The average nuclear and soma area, as well as the length and number of neurites of AraC/NT2N and RA/NT2N neurons were morphometrically analyzed and compared (González-Burguera et al., in press, for details). Comparison of the nuclear area between neurons committed to differentiate with either RA or AraC showed that nuclei of AraC/NT2N neurons (339.78 ± 12.03 µm^2) were 3.2-fold larger than those of RA/NT2N neurons (106.83 ± 12.03 µm^2). Similarly, the average soma area of AraC/NT2N neurons (1103.15 ± 41.69 µm^2) was about 4.6-fold larger compared to that of RA/NT2N neurons (240.17 ± 9.93 µm^2). Consequently, the ratio of nuclear to body area tended to equalize in both phenotypes, although it was significantly lower in AraC/NT2N (0.344 ± 0.017) than in RA/NT2N (0.483 ± 0.015) neurons. Neurites of AraC/NT2N neurons were 105.33 ± 3.55 µm long in average, which represents about half the value found in RA/NT2N neurons (225.46 ± 10.94 µm). This, together with a slightly lower, non-significant, number of neurites per cell in AraC/NT2N (1.85 ± 0.10) than in RA/NT2 neurons (2.12 ± 0.13), makes total arborization 2.2-fold longer in RA/NT2N (390.70 ± 17.89 µm) than in AraC/NT2N (180.14 ± 9.22 µm). These data showing comparisons between the morphometric parameters measured in AraC/NT2N and RA/NT2N cells are presented in González-Burguera et al. (in press); Fig. 1K).

3.4. AraC/NT2N co-express glutamatergic and cholinergic phenotypic markers

The expression of specific markers for glutamatergic, cholinergic, GABAergic, and dopaminergic neurotransmitter phenotypes was first

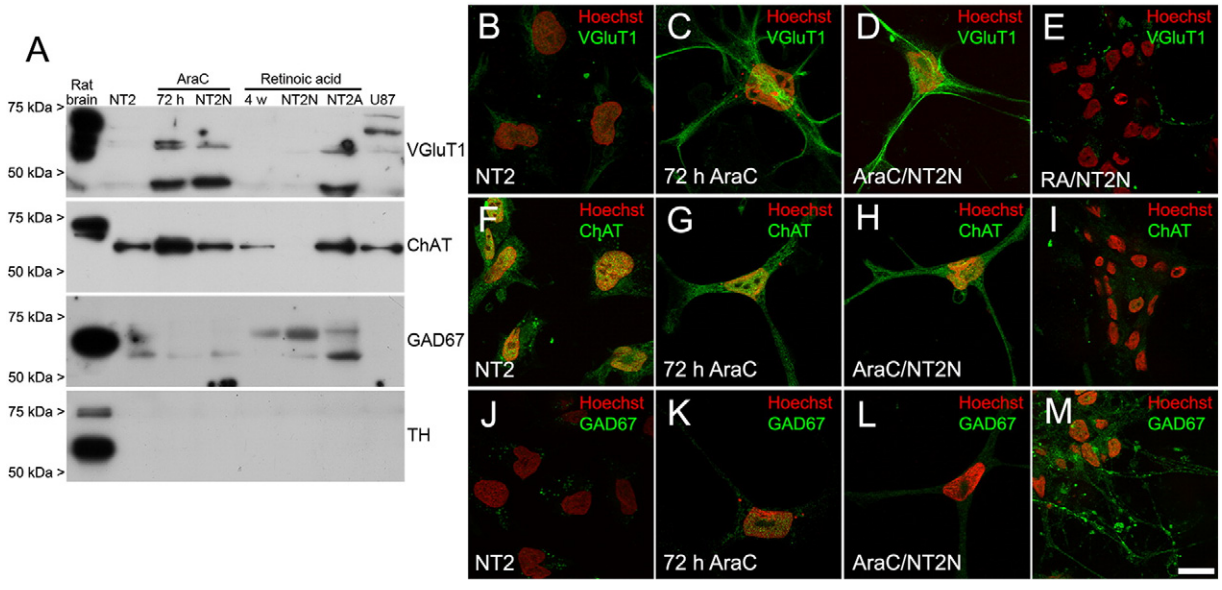

Fig. 4. (A) Western blot analysis of neurotransmitter phenotype markers in total cell lysates from NT2 cells (20 µg) during the RA- and AraC-induced differentiation. Rat brain homogenates (4 µg) and human U87 glioma cell line lysates (20 µg) were used as positive and negative controls, respectively. Specific antibodies to vesicular glutamate transporter 1 (VGluT1), choline acetyl transferase (ChAT), glutamate decarboxylase 67 kDa (GAD67), and tyrosine hydroxylase (TH) enzymes were used as glutamatergic, cholinergic, GABAergic, and dopaminergic phenotype markers. (B–M) Immunolabeling (green) against VGluT1 (A–E), ChAT (F–I), and GAD67 (J–M) combined with Hoechst's chromatin staining (pseudocolored red) in fixed NT2 cells, cells treated for 72 h with AraC, and AraC/NT2N and RA/NT2N neurons. Micrographs are maximum intensity projections of 3 consecutive optical sections separated by 0.24 µm, obtained by structured illumination microscopy (ApoTome). Scale bar = 20 µm (applies to B-M).

analyzed in homogenates from AraC- and RA-treated NT2 cultures. For this purpose, we used specific antibodies to vesicular glutamate transporter 1 (VGluT1), choline acetyl transferase (ChAT), and glutamate decarboxylase 67 kDa (GAD67) and tyrosine hydroxylase (TH) enzymes. In rat brain homogenates, used as positive controls, all four antibodies produced immunoreactive bands (Fig. 4A), consistent with the size predicted from the corresponding rat protein sequences. Results obtained in cell homogenates revealed marked differences between AraC- and RA-treated cells. Briefly, high VGluT1 and ChAT immunoreactivity was observed in AraC-differentiated NT2N cells, whereas strong GAD67- and barely detectable VGluT1 immunoreactivity was detected in RA-differentiated NT2N cells. We found no TH immunoreactivity in any of the cell samples analyzed even after overexposure of western blots (Fig. 4A) (see supplementary results for a detailed description of western blot results and related discussion).

In agreement with the results of western blot analysis, NT2 progenitors exhibited barely detectable VGluT1 immunofluorescence (Fig. 4B), whereas bright staining was detected throughout cells processes of cells differentiated into neurons by AraC treatment for 72 h and 6 days (Figs. 4C and D). In the same immunocytochemical staining conditions, VGluT1-signal was seen as bright foci restricted to varicosities on a small subset of neurites of RA/NT2N cells (Fig. 4E). ChAT immunoreactivity was diffusely distributed throughout the cytoplasm of NT2 progenitors (Fig. 4F) and extended to neurites of AraC-differentiated cells (Figs. 4G–H), but no signal above the background level was detected in RA/NT2N neurons (Fig. 4I). NT2 progenitors (Fig. 4J), and AraC-treated cells (Figs. 4K–L) were nearly devoid of GAD67 immunofluorescence staining, whereas most neurites of RA/NT2N cell displayed bright staining (Fig. 4M). Immunofluorescence staining showed that virtually all AraC/NT2N neurons were both VGluT1- and ChAT-immunopositive, strongly indicating that these cells co-express glutamatergic and cholinergic markers. Thus, we carried out double VGluT1/ChAT immunofluorescence staining, showing that every VGluT1-positive neuron also expressed ChAT (Fig. 5A). Although both markers were distributed in neurites of AraC/NT2N cells, VGluT1 immunofluorescence was highly polarized to neurites, whereas anti-ChAT antibody also stained flat lamellipodia (Figs. 5B–D). Because cells committed to differentiate into neurons by AraC treatment cannot be physically separated from non-neuronal cells for western blot analysis, immunofluorescence analysis allowed us to compare these two cell phenotypes with respect to the expression of VGluT1 and ChAT. VGluT1 immunoreactivity in flat polygonal non-neuronal cells (Figs. 5B–D, stars) was mostly restricted to perinuclear locations (Fig. 5B), whereas ChAT-staining extended further to the whole cytoplasm (Fig. 5C), even delineating the whole cellular perimeter.

3.5. AraC/NT2 neurons are irreversibly postmitotic

Cell proliferation was assessed by BrdU incorporation and cell counting during the time course AraC-induced neuronal differentiation. About three-quarters (75.32 ± 1.32%) of NT2 progenitors incorporated BrdU after a 4-h pulse prior to fixation (Figs. 6A, F). Treatment with AraC rapidly inhibited DNA replication. Thus, in NT2 cells incubated with BrdU during the first 4 h of AraC treatment, the proportion of BrdU-immunopositive cells felt to less than half (48.90 ± 1.59%) (Figs. 6B, F) and decreased steadily during the next 12 h of AraC treatment (Figs. 6C–E, F), such that no BrdU-immunopositive cells were detected after this time point.

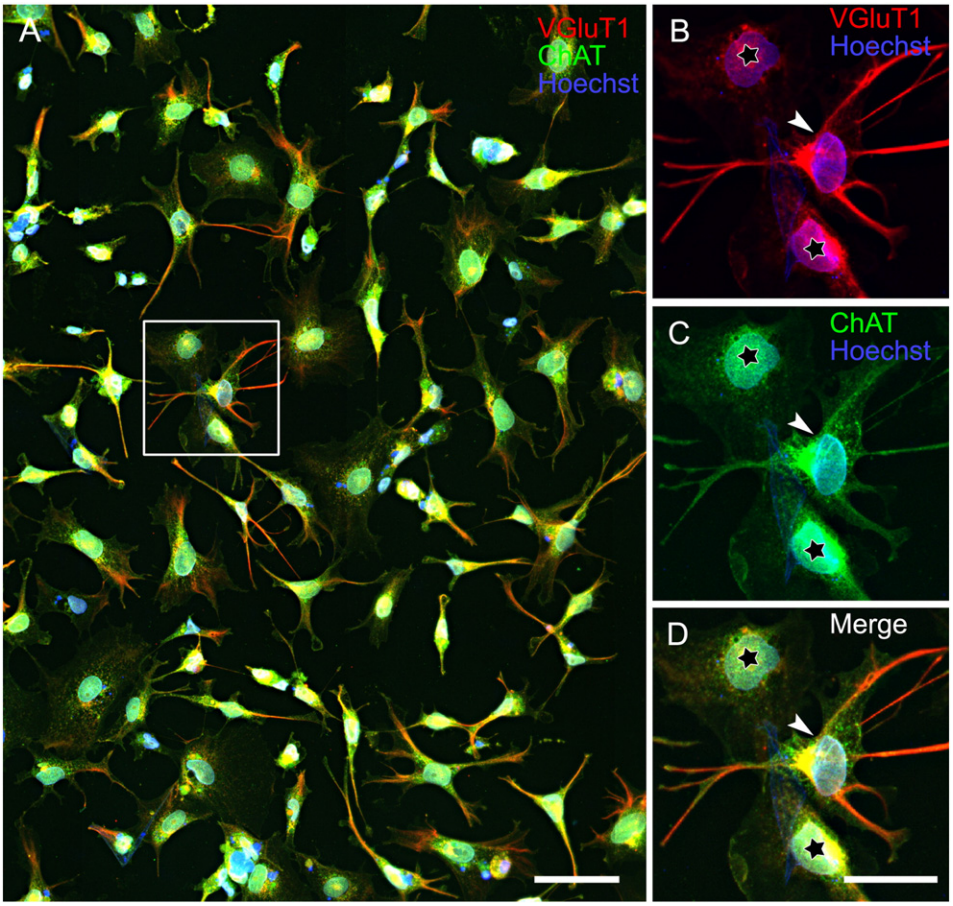

Fig. 5. Epifluorescence microscopy images of AraC/NT2N cells processed for double immunofluorescence to VGluT1 (red) and ChAT (red) combined with Hoechst's staining (blue). (A) Panoramic view corresponding to a mosaic from multiple images captured with a 20× objective. (B–D) Higher magnification of the area framed in A for a better view of VGluT1 (B) and ChAT immunofluorescence (C) distribution in an AraC/NT2N neuron (arrowhead) and in non-neuronal cells (stars). Scale bars = 100 μm in A; 50 μm in D.

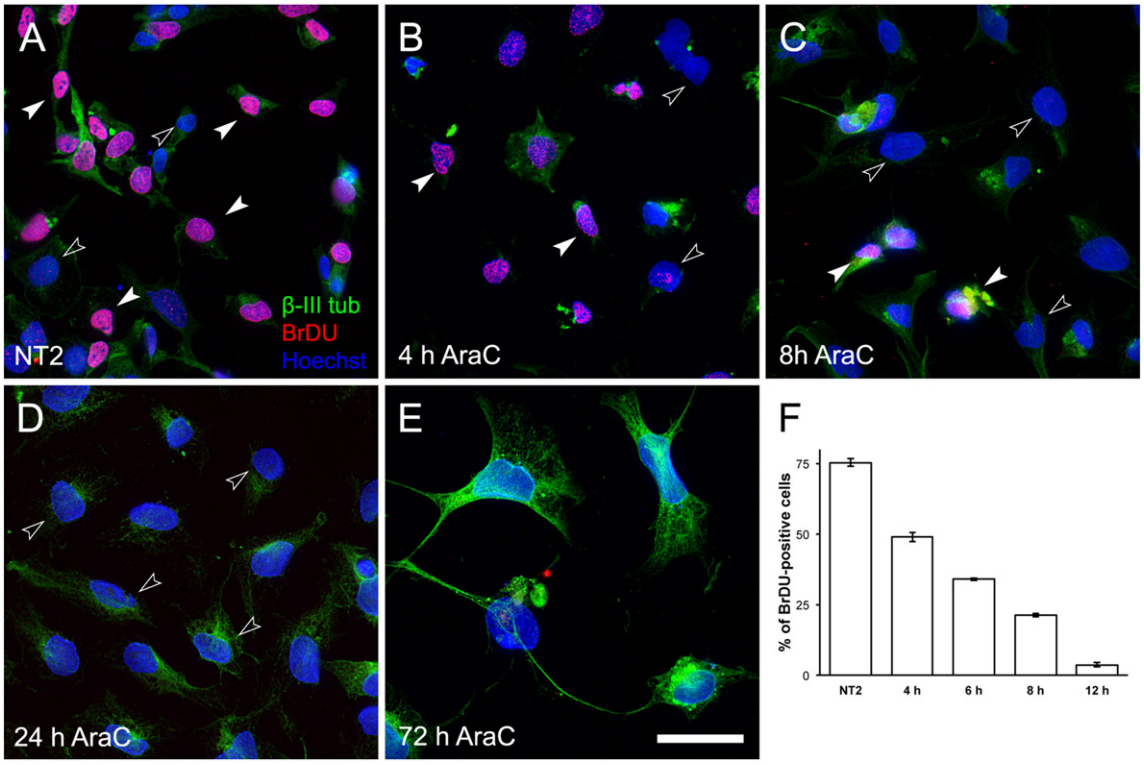

Fig. 6. (A–D) Epifluorescence microscopy images of NT2 cells subjected to 4-h BrdU pulses during the time course of AraC-induced differentiation and processed for double immunofluorescence against BrdU (red) and β-III tubulin (green), combined with Hoechst's chromatin staining (blue). Filled and empty arrowheads correspond to BrdU-positive and BrdU-negative cells. Scale bar = 50 μm (applies to A–D). (G) Bar graphs showing results of BrdU incorporation analysis during the time course of AraC-induced differentiation of NT2 cells. Data represent mean ± SEM from three independent experiments.

To assess whether cell division arrest caused by AraC treatment was reversible, AraC-containing medium was replaced with fresh complete medium after the 6-day period of treatment, and cells were subjected to 4-h BrdU pulses before fixation at different time points. Cells fixed 24, 48, or 96 h after removal of AraC failed to incorporate BrdU (Fig. S5), strongly suggesting that AraC/NT2 cells are postmitotic and unable to return to a premitotic state. Noticeably, cell viability decreased rapidly after removal of AraC, such that only a few cells (<100/slide) remained viable by day 5. To rule out that failure of BrdU incorporation after 4-h pulses was caused by a slowdown in cell cycle progression, additional experiments were performed in cell cultures fixed at the same time points, but exposed to BrdU during 24 h before fixation. Again, no BrdU labeling was detected in these conditions (Fig. S5), demonstrating that AraC/NT2 neurons are irreversibly postmitotic.

4. Discussion

NT2 derived neuronal cells *in vitro* express a plethora of neuron-specific markers at both transcript and protein levels (Pleasure et al., 1992; Cheung et al., 1999; Megiorni et al., 2005; Couillard-Despres et al., 2008; Haile et al., 2014). Our results are roughly in line with previous studies showing increased expression of NF200 (Lee and Andrews, 1986; Pleasure et al., 1992), β-III tubulin (Megiorni et al., 2005; Couillard-Despres et al., 2008; Popovic et al., 2014), and DCX during RA-induced differentiation (Couillard-Despres et al., 2008). However, differences in culture conditions and the lack of data of the time course expression (or election of unequal time points for analysis) in these studies make it difficult a reliable comparison between their and our results. An inherent limitation for interpretation of results arises from the heterogeneous composition of cultures during RA-induced differentiation. Indeed, the neuronal phenotype represents only a small fraction over the entire cell population before mechanical isolation of RA/NT2N cells. Of the three markers used, NF200 was clearly identified as a highly neuron-specific marker in terminal cultures, in view of the high enrichment in this protein in terminally differentiated RA/NT2N cells compared to cell samples harvested before mechanical dislodging of neuronal cells. By contrast, expression levels of β-III tubulin and DCX were similar in samples from cultures after 28 days of treatment and in those from terminally differentiated RA/NT2N cells, indicating that these proteins were expressed in both RA/NT2N neurons and in the highly adherent non-neuronal NT2A cells. Remarkably, β-III tubulin was already detectable in NT2 cells, reached a maximum immunoreactivity by day 7 of RA treatment, and returned to basal levels at the end of the process. This is in agreement with a similar time course analysis performed by Megiorni et al. (2005), even thought they used a cell aggregation method that shortens the time of the RA-induced differentiation to 3–4 weeks. Collectively, these data support and extend previous findings of the expression of neuronal markers in RA/NT2N neurons and emphasizes the caution needed in drawing conclusions about the use of β-III tubulin for an unequivocal identification of neuronal phenotypes. In line with this conclusion, β-III tubulin is expressed in human fetal astrocytes (Dráberová et al., 2008) as well as in undifferentiated mesenchymal stem cells (Foudah et al., 2014). Our findings show that NT2N cells derived from AraC treatment not only show neuronal morphology, but also express neuronal markers, albeit with remarkable differences in the expression profiles of β-III tubulin and DCX during differentiation. At difference with that observed during RA-induced differentiation, in AraC-treated cultures, immunoreactivity for β-III tubulin increased sharply at mid-treatment and reached a maximum at day 6, whereas DCX showed an up-down regulation pattern that peaked up at 48 h post-treatment. The progressive increase in expression of NeuN/Fox-3 observed during AraC-induced differentiation of NT2 progenitors, as analyzed by western blot and immunofluorescence microscopy, further confirmed the neuronal identity of AraC/NT2N neurons. The sequential and non-matching upregulation of the early (Brown et al., 2003) and late (Mullen et al., 1992) neuronal markers DCX and

NeuN/Fox-3 suggests that, beside differentiation, AraC/NT2N cells have begun a maturation process after 6 days of treatment. However, this suggestion should be considered with caution, as NeuN/Fox-3 expression has been found in non-neuronal cells, such as cultured rodent and human astrocytes and even 3T3 fibroblast cells (Darlington et al., 2008). Indeed, we also observed that part of the population of non-neuronal flat polygonal cells in our AraC-treated terminal cultures displayed weak to moderate nuclear staining for NeuN/Fox-3, leading us to consider morphological features to classify cells into non-neuronal or AraC/NT2N neuronal. Less than 10% of the cells in culture survived the uninterrupted 6-day period of AraC treatment, and only about 50% of them fulfilled the double criterion to be considered as neuronal (i.e., NeuN/Fox-3 positive nucleus and presence of neurite extensions) leading to a differentiation efficiency similar to that found after RA-differentiation. Our modified procedure, consisting of increasing cell density at mid-treatment, doubled overall cell survival and increased the percentage of neuronal cells with respect the total population at the end of AraC treatment to 71%, respectively. Consequently, differentiation efficiency was number augmented by almost 3-fold.

The two populations identified were clearly distinguishable as demonstrated by morphometric measurements of cell nuclei and total cell area. When compared with RA/NT2N neurons, AraC/NT2N neurons displayed considerably larger nuclei and cell somata, although the ratio of nuclear area to body area tended to get closer in both phenotypes, but still significantly lower in AraC/NT2N neurons. An overestimation of the size of cell somata of AraC/NT2N neurons, due to limitations on accurately defining their boundaries of (González-Burguera et al., in press), could account for this difference. Morphometric analysis of neurites showed that AraC/NT2N neurons displayed an average neurite length of about 105 μm, which corresponds to less than half the length of 225 μm observed in RA/NT2 neurons. This value is consistent with data by Haile et al. (2014), which reported an average neurite length of about 240 μm in RA/NT2N neurons. However, because the average number of RA/NT2N neurites reported by Haile et al. (2014) was about 1.5-fold higher, the total neurite length per cell (about 759 μm) observed by these authors was almost double as compared with our data (about 390 μm). Either way, our measurements show a 2.2-fold greater total arborization length for RA/NT2N than for AraC/NT2N neurons. The much shorter time period for neurite outgrowth in AraC/NT2N neurons likely accounts for this difference. Indeed, AraC/NT2N neurons were enriched in lamellar extensions and filopodia-like processes, indicative of intensive neurite outgrowth activity. In support of this idea, neurite length found here was about 20% longer than that reported by Tegenge et al. (2011) in RA-differentiated neurons using the shortened cell aggregation method described by Cheung et al. (1999). Hence, longer survival periods would be probably required for AraC-differentiated neurons to develop longer neurite arborizations. However, under the present culture conditions, the reduction in cell viability observed after the end of the 6-day period of AraC treatment did not allow such a long-term analysis. Therefore, increasing stability of AraC/NT2 neurons by testing different culture conditions (including media, growth factors, matrices, and/or co-culture with astrocytes) will be one of the major challenges for future. Whatever the case, the experimental results reported here reveal that NT2 progenitors can be committed to differentiate in a short time period and with high efficiency into postmitotic neurons (as demonstrated by BrdU incorporation assays), and underline that AraC-induced differentiation of NT2 cells represents a valuable model to study molecular mechanisms underlying neuronal differentiation.

RA/NT2N neurons have been shown to express a broad spectrum of neurotransmitter markers *in vitro*, including glutamatergic (Podrygajlo et al., 2009; Coyle et al., 2011), cholinergic (Guillemain et al., 2000; Saporta et al., 2000), GABAergic (Yoshioka et al., 1997; Guillemain et al., 2000; Saporta et al., 2000; Podrygajlo et al., 2009; Coyle et al., 2011), catecholaminergic (Guillemain et al., 2000; Saporta et al., 2000), and serotonergic (Podrygajlo et al., 2009) transcripts and/or proteins. The apparent absence of consensus on the final neurotransmitter phenotype can be attributed to differences in the neuronal differentiation protocol and culture conditions, although as discussed by Podrygajlo et al. (2009), passage number of precursors, or their genetic instability could also contribute to variability of results. Nevertheless, under the culture conditions (culture media included) described by Pleasure et al. (1992) and used here, Yoshioka et al. (1997) and Guillemain et al. (2000) reported that a considerable population of neurons possess a GABAergic phenotype, in agreement with our findings showing that RA/NT2 are mostly GABAergic. In their immunocytochemistry-based study, Guillemain et al. (2000) found that 66.5% of neurons were GABA-immunopositive, although they also reported that 51.8% and 49.5% of neurons were TH- and ChAT-immunoreactive, respectively, leading to the conclusion that many neurons were immunopositive for at least two markers. For their part, Yoshioka et al. (1997) only analyzed GAD67 transcript and protein using RT-PCR and western blot analysis. Here, using immunofluorescence microscopy, we observed a large amount of GAD67-immunopositive and scarce VGluT1-immunopositive thin neurites, both likely corresponding to axons; hence, to the canonical distribution of these proteins. Although, due to this distribution pattern, we could not asses the proportion of neurons of each phenotype, western blot analysis confirmed that, in our culture conditions, GABA is the major neurotransmitter in RA/NT2N cells, whereas only a weak VGluT1 signal could be observed.

Of particular interest in the present report is the finding that cells committed to differentiate by short treatment with AraC displayed a completely different neurotransmitter phenotype when compared with RA/NT2N neurons. Western blot analysis showed strong immunoreactivity for VGluT1 and ChAT in samples from terminal cultures, starting as soon as 72 h after initiation of AraC treatment. On the other hand, immunofluorescence assays evidenced that virtually all terminally differentiated neurons co-expressed both markers, suggesting that their neurotransmitter phenotype was not fully defined. Noticeably, this same phenomenon has been recently described for hippocampal embryonic neural progenitors. Thus, Bhargava et al. (2010) reported that when cultures were obtained from brain of 18 days old embryos, most VGluT1-positive neurons also expressed ChAT protein. On the contrary, this ability to co-express both markers of neurotransmitter phenotype was not observed in cultures from either neonatal or adult hippocampus. Results by Bhargava et al. (2010) exemplify the importance of tissue environmental signals in specification of neurotransmitter fate. Moreover, embryonic hippocampal neurons in culture express the late neuronal marker NeuN/Fox-3 (Taguchi et al., 2014), indicating that neuronal maturation and specification of neurotransmitter phenotype are separate developmental events. As discussed by Bhargava et al. (2010), a complex combinational strategy of electrochemical coding that involves neighboring environmental signals, as well as distant afferent and retrograde signals, appear to account for specification of neurotransmitter phenotype (Johnson, 1994; Asmus et al., 2000; Landis, 2002). As a result of this developmental process, neurons would loss the ability to synthesize multiple neurotransmitters. In this regard, it is likely that AraC/NT2N cells could acquire a specific neurotransmitter phenotype when engrafted in brain. In support of this, previous studies have demonstrated that RA/NT2N neurons (Saporta et al., 2000) and even NT2 progenitors (Miyazono et al., 1996) transplanted in different regions of the rodent brain are driven to differentiate in specific neurotransmitter phenotypes according to local environmental cues. Although some experimental studies using RA/NT2N grafts in animal models of stroke (Borlongan et al., 1998a, 1998b; Saporta et al., 1999) and Huntington's disease (Hurlbert et al., 1999) have yielded promising results, others have reported either limited improvement (Bliss et al., 2006), or no effects on behavior or neurological function (Baker et al., 2000; Zhang et al., 2005; Bliss et al., 2006), which has been attributed, at least in part, to the low amount of neurons of the desired neurotransmitter phenotype,

which is a key prerequisite for successful neuronal replacement. Future studies will disclose whether AraC/NT2N cells are a suitable source of glutamatergic and cholinergic neurons for replacement of cortical excitatory neurons and basal forebrain cholinergic neurons in animal models of ischemic insult and Alzheimer's disease.

Acknowledgments

This work was supported by grants of the Basque Government (GIC/IT-589/13, SAIOTEK S-PE11UN124-125 and DKR-2012-59 to A. R.), the University of the Basque Country (UPV/EHU 243/2011 to I. G-B.), and the Instituto de Salud Carlos III, Centro de Investigación Biomédica en Red de Salud Mental, CIBERSAM. The funders had no role in study design, data collection and analysis, decision to publish, or preparation of the manuscript. No potential conflicts of interest were disclosed.

Appendix A. Supplementary data

Supplementary data to this article can be found online at http://dx.doi.org/10.1016/j.scr.2016.02.038.

References

Andrews, P.W., 1984. Retinoic acid induces neuronal differentiation of a cloned human embryonal carcinoma cell line in vitro. Dev. Biol. 103, 285–293. http://dx.doi.org/10.1016/0012-1606(84)90316-6.

Asmus, S.E., Parsons, S., Landis, S.C., 2000. Developmental changes in the transmitter properties of sympathetic neurons that innervate the periosteum. J. Neurosci. 20, 1495–1504.

Baker, K.A., Mendez, I., 2005. Long distance selective fiber outgrowth of transplanted hNT neurons in white matter tracts of the adult rat brain. J. Comp. Neurol. 486, 318–330. http://dx.doi.org/10.1002/cne.20477.

Baker, K.A., Hong, M., Sadi, D., Mendez, I., 2000. Intrastriatal and intranigral grafting of hNT neurons in the 6-OHDA rat model of Parkinson's disease. Exp. Neurol. 162, 350–360. http://dx.doi.org/10.1006/exnr.1999.7337.

Banerjee, S., Williamson, D., Habib, N., Gordon, M., Chataway, J., 2010. Human stem cell therapy in ischaemic stroke: a review. Age Ageing 40, 7–13. http://dx.doi.org/10.1093/ageing/afq133.

Bhargava, N., Das, M., Edwards, D., Stancescu, M., Kang, J.F., Hickman, J.J., 2010. Coexpression of glutamate vesicular transporter (VGLUT1) and choline acetyltransferase (ChAT) proteins in fetal rat hippocampal neurons in culture. In Vitro Cell. Dev. Biol. Anim. 46, 685–692. http://dx.doi.org/10.1007/s11626-010-9324-0.

Bliss, T.M., Kelly, S., Shah, A.K., Foo, W.C., Kohli, P., Stokes, C., Sun, G.H., Ma, M., Masel, J., Kleppner, S.R., Schallert, T., Palmer, T., Steinberg, G.K., 2006. Transplantation of hNT neurons into the ischemic cortex: cell survival and effect on sensorimotor behavior. J. Neurosci. Res. 83, 1004–1014. http://dx.doi.org/10.1002/jnr.20800.

Borlongan, C.V., Saporta, S., Poulos, S.G., Othberg, A., Sanberg, P.R., 1998a. Viability and survival of hNT neurons determine degree of functional recovery in grafted ischemic rats. Neuroreport 9, 2837–2842. http://dx.doi.org/10.1097/00001756-199808240-00028.

Borlongan, C.V., Tajima, Y., Trojanowski, J.Q., Lee, V.M.-Y., Sanberg, P.R., 1998b. Transplantation of cryopreserved human embryonal carcinoma-derived neurons (NT2N cells) promotes functional recovery in ischemic rats. Exp. Neurol. 149, 310–321. http://dx.doi.org/10.1006/exnr.1997.6730.

Borlongan, C.V., Fournier, C., Stahl, C.E., Yu, G., Xu, L., Matsukawa, N., Newman, M., Yasuhara, T., Hara, K., Hess, D.C., Sanberg, P.R., 2006. Gene therapy, cell transplantation and stroke. Front. Biosci. 11, 1090–1101.

Brown, J.P., Couillard-Despres, S., Cooper-Kuhn, C.M., Winkler, J., Aigner, L., Kuhn, H.G., 2003. Transient expression of doublecortin during adult neurogenesis. J. Comp. Neurol. 467, 1–10. http://dx.doi.org/10.1002/cne.10874.

Cheung, W.M., Fu, W.Y., Hui, W.S., Ip, N.Y., 1999. Production of human CNS neurons from embryonal carcinoma cells using a cell aggregation method. Biotechniques 26 (5), 946–948.

Couillard-Despres, S., Quehl, E., Altendorfer, K., Karl, C., Ploetz, S., Bogdahn, U., Winkler, J., Aigner, L., 2008. Human in vitro reporter model of neuronal development and early differentiation processes. BMC Neurosci. 9 (31). http://dx.doi.org/10.1186/1471–2202-9-31.

Coyle, D.E., Li, J., Baccei, M., 2011. Regional differentiation of retinoic acid-induced human pluripotent embryonic carcinoma stem cell neurons. PLoS One 6, e16174. http://dx.doi.org/10.1371/journal.pone.0016174.

Darlington, P.J., Goldman, J.S., Cui, Q.L., Antel, J.P., Kennedy, T.E., 2008. Widespread immunoreactivity for neuronal nuclei in cultured human and rodent astrocytes. J. Neurochem. 104, 1201–1209. http://dx.doi.org/10.1111/j.1471-4159.2007.05043.x.

Dráberová, E., Del Valle, L., Gordon, J., Marková, V., Smejkalová, B., Bertrand, L., de Chadarévian, J.P., Agamanolis, D.P., Legido, A., Khalili, K., Dráber, P., Katsetos, C.D., 2008. Class III beta-tubulin is constitutively coexpressed with glial fibrillary acidic protein and nestin in midgestational human fetal astrocytes: implications for phenotypic identity. J. Neuropathol. Exp. Neurol. 67, 341–354. http://dx.doi.org/10.1097/NEN.0b013e31816a686d.

Foudah, D., Monfrini, M., Donzelli, E., Niada, S., Brini, A.T., Orciani, M., Tredici, G., Miloso, M., 2014. Expression of neural markers by undifferentiated mesenchymal-like stem cells from different sources. J. Immunol. Res. 2014, 987678. http://dx.doi.org/10.1155/2014/987678.

González-Burguera, I., Ricobaraza, A., Aretxabala, X., Barrondo, S., García del Caño, G., López de Jesús, M., Sallés, J., 2016. Data Supporting Morphometric Characterization of NT2-Derived Postmitotic Neurons Data in Brief. in press.

Guillemain, I., Alonso, G., Patey, G., Privat, A., Chaudieu, I., 2000. Human NT2 neurons express a large variety of neurotransmission phenotypes in vitro. J. Comp. Neurol. 422, 380–395. http://dx.doi.org/10.1002/1096-9861(20000703)422:3<380::AID-CNE5>3.0.CO;2-C.

Haile, Y., Fu, W., Shi, B., Westaway, D., Baker, G., Jhamandas, J., Giuliani, F., 2014. Characterization of the NT2-derived neuronal and astrocytic cell lines as alternative in vitro models for primary human neurons and astrocytes. J. Neurosci. Res. 92, 1187–1198. http://dx.doi.org/10.1002/jnr.23399.

Hara, K., Yasuhara, T., Maki, M., Matsukawa, N., Masuda, T., Yu, S.J., Ali, M., Yu, G., Xu, L., Kim, S.U., Hess, D.C., Borlongan, C.V., 2008. Neural progenitor NT2N cell lines from teratocarcinoma for transplantation therapy in stroke. Prog. Neurobiol. 85, 318–334. http://dx.doi.org/10.1016/j.pneurobio.2008.04.005.

Hartley, R.S., Margulis, M., Fishman, P.S., Lee, V.M., Tang, C.M., 1999a. Functional synapses are formed between human NTera2 (NT2N, hNT) neurons grown on astrocytes. J. Comp. Neurol. 407, 1–10. http://dx.doi.org/10.1002/(SICI)1096-9861(19990428)407:1<1::AID-CNE1>3.0.CO;2-Z.

Hartley, R.S., Trojanowski, J.Q., Lee, V.M., 1999b. Differential effects of spinal cord gray and white matter on process outgrowth from grafted human NTERA2 neurons (NT2N, hNT). J. Comp. Neurol. 415, 404–418. http://dx.doi.org/10.1002/(SICI)1096-9861(19991220)415:3<404::AID-CNE6>3.0.CO;2-R.

Hurlbert, M.S., Gianani, R.I., Hutt, C., Freed, C.R., Kaddis, F.G., 1999. Neural transplantation of hNT neurons for Huntington's disease. Cell Transplant. 8, 143–151.

Miyazono, M., Nowell, P.C., Finan, J.L., Lee, V.M., Trojanowski, J.Q., 1996. Long-term integration and neuronal differentiation of human embryonal carcinoma cells (NTera-2) transplanted into the caudoputamen of nude mice. J. Comp. Neurol. 376, 603–613. http://dx.doi.org/10.1002/(SICI)1096-9861(19961223)376:4<603::AID-CNE8>3.0.CO;2-5.

Johnson, M.D., 1994. Synaptic glutamate release by postnatal rat serotonergic neurons in microculture. Neuron 12, 433–442. http://dx.doi.org/10.1016/0896-6273(94)90283-6.

Kleppner, S.R., Robinson, K.A., Trojanowski, J.Q., Lee, V.M., 1995. Transplanted human neurons derived from a teratocarcinoma cell line (Ntera2) mature, integrate and survive for over 1 year in the nude mouse brain. J. Comp. Neurol. 357, 618–636. http://dx.doi.org/10.1002/cne.903570410.

Kondziolka, D., Wechsler, L., Goldstein, S., Meltzer, C., Thulborn, K.R., Gebel, J., Jannetta, P., DeCesare, S., Elder, E.M., McGrogan, M., Reitman, M.A., Bynum, L., 2000. Trasplantation of cultured human neuronal cells for patients with stroke. Neurology 55, 565–569.

Kondziolka, D., Steinberg, G.K., Wechsler, L., Meltzer, C.C., Elder, E., Gebel, J., Decesare, S., Jovin, T., Zafonte, R., Lebowitz, J., Flickinger, J.C., Tong, D., Marks, M.P., Jamieson, C., Luu, D., Bell-Stephens, T., Teraoka, J., 2005. Neurotransplantation for patients with subcortical motor stroke: a phase 2 randomized trial. J. Neurosurg. 103, 38–45.

Landis, S.C., 2002. Quick-change artist: from excitatory to inhibitory synapse in minutes. Nat. Neurosci. 5, 503–504. http://dx.doi.org/10.1038/nn0602-503.

Lee, V.M., Andrews, P.W., 1986. Differentiation of NTERA-2 clonal human embryonal carcinoma cells into neurons involves the induction of all three neurofilament proteins. J. Neurosci. 6, 514–521.

Lee, V.M., Hartley, R.S., Trojanowski, J.Q., 2000. Neurobiology of human neurons (NT2N) grafted into mouse spinal cord: implications for improving therapy of spinal cord injury. Prog. Brain Res. 128, 299–307. http://dx.doi.org/10.1016/S0079-6123(00)28027-8.

Martínez-Morales, P.L., Revilla, A., Ocaña, I., González, C., Sainz, P., McGuire, D., Liste, I., 2013. Progress in stem cell therapy for major human neurological disorders. Stem Cell Rev. 9, 685–699. http://dx.doi.org/10.1007/s12015-013-9443-6.

Megiorni, F., Mora, B., Indovina, P., Mazzilli, M.C., 2005. Expression of neuronal markers during NTera2/cloneD1 differentiation by cell aggregation method. Neurosci. Lett. 373, 105–109. http://dx.doi.org/10.1016/j.neulet.2004.09.070.

Meltzer, C.C., Kondziolka, D., Villemagne, V.L., Wechsler, L., Goldstein, S., Thurlborn, K.R., Gebel, J., Elder, E.M., DeCesare, S., Jacobs, S., 2001. Serial [18F] fluorodeoxyglucose positron emission tomography after human neuronal implantation for stroke. Neurosurgery 49, 586–591.

Mullen, R.J., Buck, C.R., Smith, A.M., 1992. NeuN, a neuronal specific nuclear protein in vertebrates. Development 116, 201–211.

Musch, T., Öz, Y., Lyko, F., Breiling, A., 2010. Nucleoside drugs induce cellular differentiation by caspase-dependent degradation of stem cell factors. PLoS One 5, e10726. http://dx.doi.org/10.1371/journal.pone.0010726.

Nelson, P.T., Kondziolka, D., Wechsler, L., Goldstein, S., Gebel, J., DeCesare, S., Elder, E.M., Zhang, P.J., Jacobs, A., McGrogan, M., Lee, V.M., Trojanowski, J.Q., 2002. Clonal human (hNT) neuron grafts for stroke therapy: neuropathology in a patient 27 months after implantation. Am. J. Pathol. 160, 1201–1206. http://dx.doi.org/10.1016/S0002-9440(10)62546-1.

Öz, S., Maercker, C., Breiling, A., 2013. Embryonic carcinoma cells show specific dielectric resistance profiles during induced differentiation. PLoS One 8, e59895. http://dx.doi.org/10.1371/journal.pone.

Pleasure, S.J., Page, C., Lee, V.M., 1992. Pure, postmitotic, polarized human neurons derived from NTera 2 cells provide a system for expressing exogenous proteins in terminally differentiated neurons. J. Neurosci. 12, 1802–1815.

Podrygajlo, G., Tegenge, M.A., Gierse, A., Paquet-Durand, F., Tan, S., Bicker, G., Stern, M., 2009. Cellular phenotypes of human model neurons (NT2) after differentiation in aggregate culture. Cell Tissue Res. 336, 439–452. http://dx.doi.org/10.1007/s00441-009-0783-0.

Podrygajlo, G., Song, Y., Schlesinger, F., Krampfl, K., Bicker, G., 2010. Synaptic currents and transmitter responses in human NT2 neurons differentiated in aggregate culture. Neurosci. Lett. 468, 207–210. http://dx.doi.org/10.1016/j.neulet.2009.10.092.

Popovic, J., Stanisavljevic, D., Schwirtlich, M., Klajn, A., Marjanovic, J., Stevanovic, M., 2014. Expression analysis of SOX14 during retinoic acid induced neural differentiation of embryonal carcinoma cells and assessment of the effect of its ectopic expression on SOXB members in HeLa cells. PLoS One 9, e91852. http://dx.doi.org/10.1371/journal.pone.0091852.

Saporta, S., Borlongan, C.V., Sanberg, P.R., 1999. Neural transplantation of human neuroteratocarcinoma (hNT) neurons into ischemic rats. A quantitative dose–response analysis of cell survival and behavioral recovery. Neuroscience 91, 519–525. http://dx.doi.org/10.1016/S0306-4522(98)00610-1.

Saporta, S., Willing, A.E., Colina, L.O., Zigova, T., Milliken, M., Daadi, M.M., Sanberg, P.R., 2000. In vitro and in vivo characterization of hNT neuron neurotransmitter phenotypes. Brain Res. Bull. 53, 263–268. http://dx.doi.org/10.1016/S0361-9230(00)00329-4.

Solovei, I., Schermelleh, L., Albiez, H., Cremer, T., 2006. Chapter 35—Detection of cell cycle stages in situ in growing cell populations. In: Celis, J.E. (Ed.), Cell Biology, third ed. Academic Press, Burlington, pp. 291–299.

Taguchi, K., Watanabe, Y., Tsujimura, A., Tatebe, H., Miyata, S., Tokuda, T., Mizuno, T., Tanaka, M., 2014. Differential expression of alpha-synuclein in hippocampal neurons. PLoS One 9, e89327. http://dx.doi.org/10.1371/journal.pone.0089327.

Tan, J., Yang, X., Zhuang, L., Jiang, X., Chen, W., Lee, P.L., Karuturi, R.K., Tan, P.B., Liu, E.T., Yu, Q., 2007. Pharmacologic disruption of polycomb-repressive complex 2-mediated gene repression selectively induces apoptosis in cancer cells. Genes Dev. 21, 1050–1063. http://dx.doi.org/10.1101/gad.1524107.

Tegenge, M.A., Roloff, F., Bicker, G., 2011. Rapid differentiation of human embryonal carcinoma stem cells (NT2) into neurons for neurite outgrowth analysis. Cell. Mol. Neurobiol. 31, 635–643. http://dx.doi.org/10.1007/s10571-011-9659-4.

Trojanowski, J.Q., Kleppner, S.R., Hartley, R.S., Miyazono, M., Fraser, N.W., Kesari, S., Lee, V.M.-Y., 1997. Transfectable and transplantable post-mitotic human neurons: a potential "platform" for gene therapy of nervous system diseases. Exp. Neurol. 144, 92–97. http://dx.doi.org/10.1006/exnr.1996.6393.

Trojanowski, J.Q., Mantione, J.R., Lee, J.H., Seid, D.P., You, T., Inge, L.J., Lee, V.M., 1993. Neurons derived from a human teratocarcinoma cell line establish molecular and structural polarity following transplantation into the rodent brain. Exp. Neurol. 122, 283–294. http://dx.doi.org/10.1006/exnr.1993.1128.

Yoshioka, A., Yudkoff, M., Pleasure, D., 1997. Expression of glutamic acid decarboxylase during human neuronal differentiation: studies using the NTera-2 culture system. Brain Res. 767, 333–339. http://dx.doi.org/10.1016/S0006-8993(97)00627-6.

Zhang, C., Saatman, K.E., Royo, N.C., Soltesz, K.M., Millard, M., Schouten, J.W., Motta, M., Hoover, R.C., McMillan, A., Watson, D.J., Lee, V.M., Trojanowski, J.Q., McIntosh, T.K., 2005. Delayed transplantation of human neurons following brain injury in rats: a long-term graft survival and behavior study. J. Neurotrauma 22, 1456–1474. http://dx.doi.org/10.1089/neu.2005.22.1456.